sciendo

POLISH MARITIME RESEARCH 4 (116) 2022 Vol. 29; pp. 4-11
10.2478/pomr-2022-0039

ANALYSIS OF MODEL-SCALE OPEN-WATER TEST UNCERTAINTY

Przemysław Król*
Maritime Advanced Research Centre, Poland
* Corresponding author: *krolprz30@gmail.com (P. Król)*

ABSTRACT

Within the frame of CTO's standard procedure, a propeller open-water test is preceded by a reference measurement, which is taken for a reference propeller model (P356). The results of these measurements are assembled to conduct an open-water test uncertainty analysis. Additional material was gathered from open-water tests that were conducted throughout several research projects on the CP469 model, which is a model of the Nawigator XXI propeller. The latter is a controllable pitch propeller; its pitch was reset before each test repetition. Known procedures for the determination of the open-water test uncertainty do not allow one to extract the manufacture impact directly, without building many models. This factor was addressed with the use of lifting surface calculations. Under certain additional assumptions, these calculations were performed for 100 generic versions of each propeller's geometry, which were generated by random deviations from the theoretical data within the limits of allowed tolerances. The results of the conducted analyses made it possible to extract separate factors, which were connected to the test's repeatability, measurement bias and geometry tolerance.

Keywords: uncertainty, propeller open-water test, lifting surface method, model-scale experiment, propulsion

INTRODUCTION

Practical ship hydromechanics is founded on a few basic experiments [1], [2] that are designed to determine the propulsion characteristics of a vessel. Providing a propulsion prognosis that is as accurate as possible is essential from a propulsion system design point of view [3], [4]. In most cases, the considered parameters (delivered power, propeller rate of revolution, etc.) are determined with an uncertainty margin that is narrow enough to provide reasonable information [5]. One of the major sources of full-scale prediction uncertainty lies in full-scale extrapolation methods [6]. Due to this, scaling procedures remain an important topic in modern studies [7], [8], including critical evaluations [9], [10]. The strong development of numerical methods has led to their application in marine propulsion problems [11], [12], [13], [14]; however, seemingly old-fashioned methods like regression formulas are still of use [15].

On the other hand, the development of theoretical (mainly numerical) methods requires the best possible empirical data for the validation of the produced models. Obviously, it is not possible to determine 'exact' parameter values through experiments, but decreasing the uncertainty of experiments makes it possible to apply a more rigorous verification of the values of constants utilised in turbulence equations, etc. In the meantime, however, it has been shown that full-scale measurement uncertainty is a complex issue – even from the point of view of the definition of input values – that is

difficult to define precisely [16]. Due to this fact, the available full-scale data can be used as reference material for theory validation only with a limited accuracy.

Thus, this work is focused on the analysis of model-scale experiments only. The main reason for this is that it allows the direct comparison of numerical methods and empirical values, with no need to transform model-scale values into full-scale values. The results of multiple repetitions of model-scale experiments and lifting surface calculations are utilised to extract particular factors that are responsible for open-water test uncertainty.

After slight modifications that address the particular case being considered, the presented methods can also be applied to the analysis of special types of propulsors like waterjets [17] or energy-saving devices [18], [19].

ANALYSED CASES

Two propeller models were investigated from a test repeatability point of view: one model has a fixed pitch (P356) and the other has a controllable pitch (CP469). The first model is a reference propeller that is tested before each set of commercial open-water tests, according to the CTO standard. The second model was utilised in several research projects.

Fig. 1. P356 (on the left) and CP469 (on the right – prepared for the tests) propeller models

The main characteristics of the abovementioned propellers are presented in Table 1.

Tab. 1. Characteristics of analysed propellers

Propeller	D_M [mm]	EAR [-]	$P_{0.7}/D$ [-]	Z [-]	Type	Blade section
P356	220.0	0.593	0.756	4	Fixed pitch	B-Wageningen
CP469	226.0	0.673	0.942	4	Controllable pitch	NACA16a08

LIFTING SURFACE ANALYSIS

The lifting surface method for open-water analysis is a classic method similar to that described in [20]. The initial step of the calculations provides a discrete representation of the propeller geometry. It is realized by determining the Cartesian coordinates of a point located on the blade profiles' mean lines at selected radial and chordwise stations. The station distribution is deduced via well-known sine and cosine formulas for radial and chordwise distributions, respectively:

$$\frac{r}{R} = \frac{r_h}{R} + \left(1 - \frac{r_h}{R}\right)\sin\frac{\pi}{2A-2}, \quad \frac{x}{c} = \frac{1}{2}\left(1 - \cos\frac{\pi}{2B-1}\right) \tag{1}$$

where r is the actual radius [m], R is the propeller radius [m], r_h is the hub radius, A is the total number of radial stations representing the propeller, x is the actual chordwise station [m], c is the chord length at the considered radius [m] and B is the total number of chordwise stations representing the propeller. An example of such a discrete representation is given in Fig. 2.

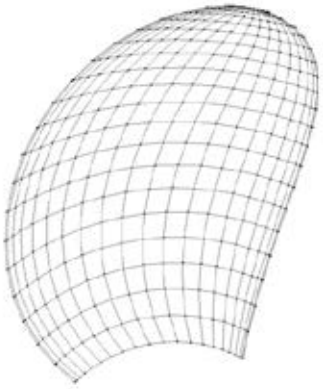

Fig. 2. Example of discrete propeller representation

Neighbouring points form a panel, and the control point and unit normal vector are determined in the middle of this panel. The panel-normal component of the external inflow vector is calculated at each control point:

$$u_n = \boldsymbol{e} \cdot (\boldsymbol{V} + 2\pi\boldsymbol{n} \times \boldsymbol{r}) \tag{2}$$

where u_n is the panel-normal velocity value [m/s], **e** is the unit vector normal to the panel surface [m], **V** is the propeller advance velocity [m/s], and **n** is the propeller rate of revolution vector [rps].

Points located on subsequent radial stations but at the same chordwise position represent the endpoints of bound vortices. These are supplemented with chordwise trailing vortices, which extend behind the blade (in theory to infinity). The vortex system is meant to represent the propeller's impact on the flow, trough-induced velocities, which are deduced via the Biot-Savart law. Initially, however, the circulation assigned to the bound vortex is unknown and has to be determined. To achieve this, a system of linear equations is constructed in such a way that it satisfies kinematic boundary conditions on the propeller surface: panel-normal velocities have to be cancelled out by velocities induced by the vortex system. Vortex circulations are taken as unknowns.

Once the circulation distribution is determined, the total local velocities on the blade surface may be determined,

and through the Kutta-Zhoukovski law, local forces may be computed:

$$\boldsymbol{L} = \boldsymbol{\rho \Gamma U_T \times \lambda} \quad (3)$$

where **L** is the lift force acting on a vortex [N], ρ is the water density [kg/m^3], Γ is the vortex circulation [m^2/s], $\mathbf{U}_T$ is the total velocity at the vortex midpoint and λ is the vortex length vector [m].

Summing up the lift forces provides the inviscid component of the hydrodynamic reaction acting on the propeller blade. The easiest way to incorporate the viscous force is to apply an additional drag force, with the value of this force being determined via an empirical formula. The results of such simulations are strongly influenced by the geometry assigned to the trailing vortices. The determination of this geometry is an important topic in itself, and researchers approach this problem cautiously [21].

The calculations in this paper were conducted under the following assumptions:

- The input geometry of the propeller is randomly variable, within manufacture tolerance limits.
- The vortex wake is considered a rigid vortex wake, with the slipstream contraction being ignored and pitch being considered the weighted mean between the propeller's geometrical pitch and advance ratio.
- The weight is calibrated to reproduce the $K_T(J)$ function resulting from the experiments; calibration is performed for an unbiased geometry,
- Viscous effects (profile drag, pressure change due to a boundary layer) are calibrated to maximize open-water efficiency agreement at the advance ratio corresponding to the efficiency peak, as the author feels that this is the best way to reproduce the propeller's dynamic behaviour.

The propeller model manufacture tolerances allowed by ITTC [22] are shown in Table 2.

Tab. 2. ITTC allowed tolerances on propeller model dimensions

Parameter	Tolerance
Diameter	0.1 mm
Pitch	0.5%
Chord	0.2 mm
Profile offsets	0.05 mm
Rake	0.005*D_M

Based on the tolerances in Table 2, 100 generic versions of both propellers were prepared through the random application of geometry deviations within the prescribed margins and investigated using lifting surface code. For each geometry (original and generic geometries), open-water calculations were performed.

PROPELLER OPEN-WATER TEST

DERIVED PARAMETERS

The basic parameters derived from propeller open-water tests are propeller loading coefficients; they are usually based on the propeller rates of revolution (K_T, K_Q) and the advance ratio *J*:

$$J = \frac{V}{nD}, \qquad K_T = \frac{T}{\rho n^2 D^4}, \quad K_Q = \frac{Q}{\rho n^2 D^5}. \quad (4)$$

Based on the complete differential method, the biases of these coefficients may be derived as follows:

$$dJ = \frac{1}{nD}\mathrm{dV} + \left|-\frac{V}{n^2 D}\mathrm{d}n\right| + \left|-\frac{V}{nD^2}\mathrm{d}D\right| \quad (5)$$

$$dK_T = \frac{1}{\rho n^2 D^4}\mathrm{dT} + \left|-\frac{T}{\rho^2 n^2 D^4}\mathrm{d}\rho\right| + \left|-\frac{2T}{\rho n^3 D^4}\mathrm{dn}\right| + \left|-\frac{4T}{\rho n^2 D^5}\mathrm{dD}\right| \quad (6)$$

$$dK_Q = \frac{1}{\rho n^2 D^5}\mathrm{dQ} + \left|-\frac{Q}{\rho^2 n^2 D^5}\mathrm{d}\rho\right| + \left|-\frac{2Q}{\rho n^3 D^5}\mathrm{dn}\right| + \left|-\frac{5Q}{\rho n^2 D^6}\mathrm{dD}\right| \quad (7)$$

Formulas defining the uncertainty of dimensionless propeller characteristics include terms referring to the diameter bias d*D*. However, this does not justify the omission of the diameter tolerance from the next step, which is the vortex analysis of the tolerance impact. Deviations in the propeller radius (and other dimensions) alter its shape and subsequently its hydrodynamic properties, as reflected by the values of the thrust *T* and torque *Q* used in Eq. (4–7). Hence, one problem is the influence of the diameter tolerance on the determined propeller loading values, and a second, separate issue is the correct calculation of dimensionless coefficients.

Once the bias is determined, the uncertainty of the loading coefficients $U_{KT/Q}$ may be derived as follows:

$$U^2_{K_{T/Q}} = dK^2_{T/Q} + P^2_{K_{T/Q}} \quad (8)$$

where the precision limit *P* is defined as [23]

$$P(M) = \frac{2S_{Dev}}{\sqrt{M}} \quad (9)$$

where S_{dev} is the standard deviation, and M is the number of measurement repetitions.

REPEATABILITY OF THE TEST

This study is based on a collection of available data gathered from CTO's database. A total of 56 repetitions of open-water tests were collected for reference propeller P356 and 14 repetitions were collected for propeller CP469. For the

controllable pitch propeller, the pitch was reset to the target value before each run.

For better insight, experimental data are given for prescribed advance ratios, which were calculated with a fourth-degree polynomial with the least-squares method.

The accuracies of the dynamometer applied during the test for each of the measured quantities that are required to determine *dKT* and *dKQ* are shown in Table 3.

Tab 3. Open-water dynamometer characteristics

dT [N]	dQ [Nm]	dn [rps]
0.263	0.0054	0.01

The tests were conducted at a rate of revolution that satisfied the critical Reynolds number Re_{cr} = 5*10^5 and reasonably covered the applied dynamometer capacity. For both propellers, the selected rate of revolution was n = 16 rps, which resulted in ratios of Re/Re_{cr} = 1.06 for P356 and Re/Re_{cr}=1.53 for CP469.

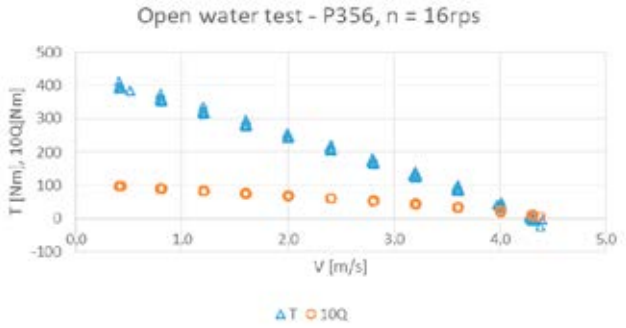

Fig. 3. Collection of measurement points for propeller P356

Table 4 contains the mean value of the thrust coefficient K_{Tm} for the corresponding advance ratio J, standard deviation S, precision limit P, bias d_{KT}, model test uncertainty U and relative value of the latter. The derived statistical parameters have small values and hence are presented after being multiplied by a factor of 100.

*Tab 4. Statistical analysis of K_T repeatability for propeller P356 at Re = 5.30*10^5*

J	*KTm*	*100S*	*100P*	*100dKT*	*100U*	*100U/KT*
0.00	0.3480	1.7147	0.4624	0.1149	0.4765	1.3690
0.10	0.3097	0.2014	0.0543	0.1046	0.1179	0.3805
0.20	0.2715	0.4916	0.1326	0.0943	0.1627	0.5993
0.30	0.2336	0.1401	0.0378	0.0841	0.0922	0.3948
0.40	0.1959	0.3355	0.0905	0.0740	0.1169	0.5966
0.50	0.1577	0.4417	0.1191	0.0637	0.1351	0.8564
0.60	0.1179	0.1960	0.0529	0.0530	0.0749	0.6352
0.70	0.0747	0.2851	0.0769	0.0414	0.0873	1.1693
0.80	0.0260	0.3491	0.0941	0.0283	0.0983	3.7752
0.90	-0.0307	0.7889	0.2128	0.0296	0.2148	-7.0005

Table 5 is constructed in a similar manner, but it contains torque-related values.

*Tab 5. Statistical analysis of K_Q repeatability for propeller P356 at Re = 5.30*10^5*

J	*KQm*	*100S*	*100P*	*100dKQ*	*100U*	*100U/KQ*
0.00	0.0394	0.1558	0.0420	0.0144	0.0444	1.1262
0.10	0.0353	0.0252	0.0068	0.0131	0.0147	0.4173
0.20	0.0317	0.0476	0.0128	0.0119	0.0175	0.5535
0.30	0.0284	0.0190	0.0051	0.0109	0.0120	0.4242
0.40	0.0252	0.0317	0.0085	0.0099	0.0131	0.5194
0.50	0.0217	0.0409	0.0110	0.0088	0.0141	0.6509
0.60	0.0177	0.0215	0.0058	0.0075	0.0095	0.5366
0.70	0.0130	0.0283	0.0076	0.0061	0.0097	0.7474
0.80	0.0073	0.0347	0.0094	0.0043	0.0103	1.4030
0.90	0.0003	0.0780	0.0210	0.0021	0.0211	60.6752

The data for propeller CP469 are presented in the same way as the data for propeller P356.

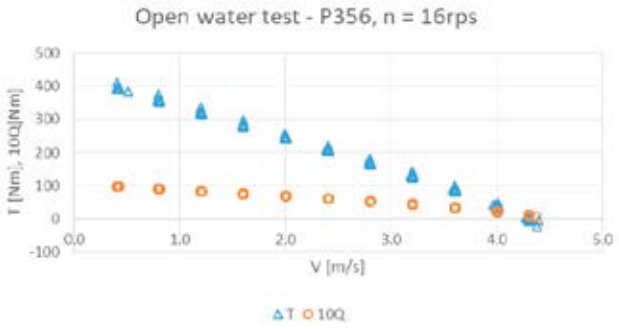

Fig. 4. Collection of measurement points for propeller CP469

Tables 6 and 7 are constructed in the same way as Tables 4 and 5, but they contain the results for propeller CP469.

*Tab. 6. Statistical analysis of K_T repeatability for propeller CP469 at Re = 7.65*10^5*

J	*KTm*	*100S*	*100P*	*100dKT*	*100U*	*100U/KT*
0.00	0.4814	0.1716	0.0952	0.1857	0.2087	0.4335
0.10	0.4344	0.1477	0.0819	0.1715	0.1901	0.4375
0.20	0.3841	0.2028	0.1125	0.1563	0.1925	0.5013
0.30	0.3323	0.2973	0.1649	0.1406	0.2167	0.6521
0.40	0.2802	0.3983	0.2209	0.1248	0.2538	0.9056
0.50	0.2282	0.4947	0.2744	0.1090	0.2953	1.2941
0.60	0.1757	0.5886	0.3265	0.0931	0.3395	1.9328
0.70	0.1214	0.6904	0.3830	0.0767	0.3906	3.2168
0.80	0.0633	0.8174	0.4534	0.0591	0.4572	7.2217
0.90	-0.0016	1.0020	0.5558	0.0404	0.5573	-349.506

*Tab. 7. Statistical analysis of K_Q repeatability for propeller CP469 at Re = 7.65*10^5*

J	KQm	100S	100P	100dKQ	100U	100U/KQ
0.00	0.0616	0.0120	0.0066	0.0250	0.0258	0.4196
0.10	0.0564	0.0142	0.0079	0.0232	0.0245	0.4340
0.20	0.0509	0.0225	0.0125	0.0213	0.0246	0.4842
0.30	0.0453	0.0321	0.0178	0.0193	0.0263	0.5800
0.40	0.0396	0.0416	0.0231	0.0173	0.0289	0.7286
0.50	0.0339	0.0508	0.0282	0.0154	0.0321	0.9461
0.60	0.0281	0.0607	0.0337	0.0134	0.0362	1.2885
0.70	0.0220	0.0732	0.0406	0.0113	0.0421	1.9106
0.80	0.0155	0.0908	0.0503	0.0090	0.0511	3.3092
0.90	0.0080	0.1180	0.0655	0.0064	0.0658	8.2336

VORTEX ANALYSIS OF TOLERANCE IMPACT

The results of vortex calculations are analysed similarly to the experimental data, with the determination of the standard deviation and precision limit based on Eq. (8) and (9). However, to emphasise the fact that these are numerical data, the precision limit from these calculations is denoted with the symbol *P*1 instead of *P*.

Tab. 8. Statistical analysis of geometry tolerance impact using vortex method for propeller model P356

J	KTm	100S1	100P1	KQm	100S1	100P1
0.00	0.3480	0.1442	0.0290	0.0396	0.0231	0.0046
0.10	0.3097	0.1263	0.0254	0.0336	0.0172	0.0035
0.20	0.2715	0.0760	0.0153	0.0294	0.0093	0.0019
0.30	0.2336	0.0449	0.0090	0.0256	0.0067	0.0013
0.40	0.1959	0.0666	0.0134	0.0219	0.0099	0.0020
0.50	0.1577	0.0840	0.0169	0.0183	0.0114	0.0023
0.60	0.1179	0.0808	0.0162	0.0147	0.0102	0.0020
0.70	0.0747	0.0669	0.0134	0.0109	0.0080	0.0016
0.80	0.0260	0.0621	0.0125	0.0129	0.0080	0.0016
0.90	-0.0307	0.0926	0.0186	-0.0018	0.0144	0.0029

Tab. 9. Statistical analysis of geometry tolerance impact using vortex method for propeller model CP469

J	KTm	100S1	100P1	KQm	100S1	100P1
0.00	0.4814	1.0733	0.2147	0.0476	0.1219	0.0244
0.10	0.4344	1.4007	0.2801	0.0509	0.1560	0.0312
0.20	0.3841	1.4725	0.2945	0.0461	0.1616	0.0323
0.30	0.3323	1.3367	0.2673	0.0402	0.1456	0.0291
0.40	0.2802	1.0891	0.2178	0.0342	0.1181	0.0236
0.50	0.2282	0.8081	0.1616	0.0285	0.0872	0.0174
0.60	0.1757	0.5457	0.1091	0.0232	0.0585	0.0117
0.70	0.1214	0.3262	0.0652	0.0176	0.0349	0.0070
0.80	0.0633	0.1501	0.0300	0.0113	0.0169	0.0034
0.90	-0.0016	0.1226	0.0245	0.0001	0.0133	0.0027

RESULTS

The precision limit value *P1*, obtained through the vortex analysis of the tolerance impact, was treated as an additional term in Eq. (8) to evaluate the overall uncertainty $U2_{KT/Q}$:

$$U2^2_{K_{T/Q}} = dK^2_{T/Q} + P^2_{K_{T/Q}} + P1^2_{K_{T/Q}} \quad (10)$$

The results of the determination of *U2* are presented in Tables 10 and 11.

Tab. 10. Overall uncertainty for propeller P356

J	KTm	100U2	U2/KT, %	KQm	100U2	U2/KQ, %
0.0000	0.3480	0.4773	1.371677	0.0394	0.0446	1.132935
0.1000	0.3097	0.1206	0.389281	0.0353	0.0152	0.429718
0.2000	0.2715	0.1634	0.601952	0.0317	0.0176	0.554577
0.3000	0.2336	0.0926	0.396586	0.0284	0.0121	0.426202
0.4000	0.1959	0.1177	0.600655	0.0252	0.0132	0.52384
0.5000	0.1577	0.1361	0.863145	0.0217	0.0143	0.65776
0.6000	0.1179	0.0766	0.64983	0.0177	0.0097	0.54744
0.7000	0.0747	0.0884	1.182838	0.0130	0.0099	0.759671
0.8000	0.0260	0.0991	3.809819	0.0073	0.0105	1.432866
0.9000	-0.0307	0.2157	-7.02451	0.0003	0.0213	71.01017

Tab. 11. Overall uncertainty for propeller CP469

J	KTm	100U2	U2/KT, %	KQm	100U2	U2/KQ, %
0.0000	0.4814	0.2994	0.621947	0.0616	0.0356	0.577137
0.1000	0.4344	0.3385	0.779214	0.0564	0.0397	0.703454
0.2000	0.3841	0.3519	0.916103	0.0509	0.0407	0.79882
0.3000	0.3323	0.3441	1.035531	0.0453	0.0392	0.865201
0.4000	0.2802	0.3344	1.193355	0.0396	0.0373	0.941435
0.5000	0.2282	0.3366	1.474966	0.0339	0.0365	1.077871
0.6000	0.1757	0.3566	2.029669	0.0281	0.0381	1.356119
0.7000	0.1214	0.3960	3.262016	0.0220	0.0427	1.941846
0.8000	0.0633	0.4582	7.238842	0.0155	0.0512	3.303988
0.9000	-0.0016	0.5578	-348.628	0.0080	0.0659	8.233411

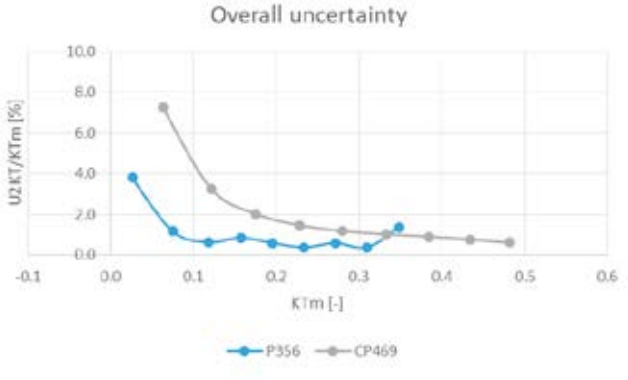

Fig. 5. Overall thrust uncertainty (100U2KT versus KT)

The influence of particular terms on the overall uncertainty is presented in the form of three factors, the test repeatability (σ), bias (ε) and geometry tolerance impact (τ):

$$\sigma = \frac{P^2}{U2^2}, \varepsilon = \frac{dK_{T/Q}^2}{U2^2}, \tau = \frac{P1^2}{U2^2} \quad (11)$$

The obtained values of these factors are shown in Tables 12 and 13.

Tab. 12. Uncertainty contributions for propeller P356

J	σT	σQ	εT	εQ	τT	τQ
0.0000	0.9384	0.8853	0.0579	0.1041	0.0037	0.01062
0.1000	0.2029	0.2010	0.7528	0.7458	0.0444	0.053238
0.2000	0.6583	0.5301	0.3329	0.4582	0.0088	0.011681
0.3000	0.1665	0.1775	0.8241	0.8109	0.0094	0.011535
0.4000	0.5915	0.4146	0.3955	0.5624	0.0130	0.022954
0.5000	0.7656	0.5939	0.2190	0.3801	0.0154	0.025966
0.6000	0.4767	0.3583	0.4785	0.5991	0.0447	0.042603
0.7000	0.7575	0.5922	0.2195	0.3815	0.0230	0.026248
0.8000	0.9025	0.8076	0.0816	0.1690	0.0159	0.023398
0.9000	0.9737	0.9718	0.0188	0.0097	0.0074	0.018532

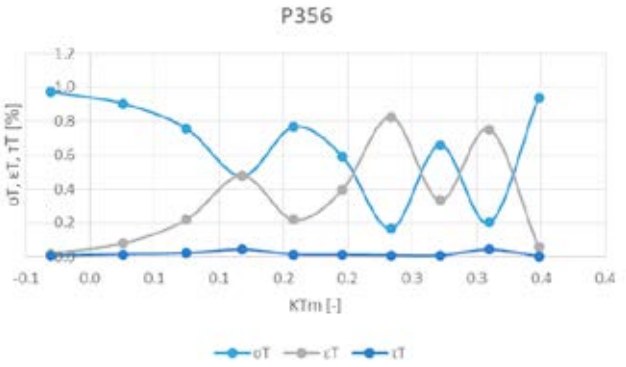

Fig. 6. Uncertainty contributions for propeller P356

Tab. 13. Uncertainty contributions for propeller CP469

J	σT	σQ	εT	εQ	τQ	τQ
0.0000	0.1011	0.0345	0.3847	0.4945	0.5142	0.471042
0.1000	0.0585	0.0396	0.2567	0.3419	0.6848	0.618414
0.2000	0.1022	0.0945	0.1973	0.2744	0.7005	0.631062
0.3000	0.2296	0.2063	0.1669	0.2425	0.6034	0.551258
0.4000	0.4364	0.3839	0.1393	0.2153	0.4243	0.400731
0.5000	0.6646	0.5956	0.1049	0.1776	0.2305	0.226759
0.6000	0.8382	0.7821	0.0682	0.1237	0.0936	0.094268
0.7000	0.9354	0.9032	0.0375	0.0700	0.0271	0.026849
0.8000	0.9791	0.9647	0.0166	0.0309	0.0043	0.004408
0.9000	0.9928	0.9889	0.0052	0.0094	0.0019	0.00168

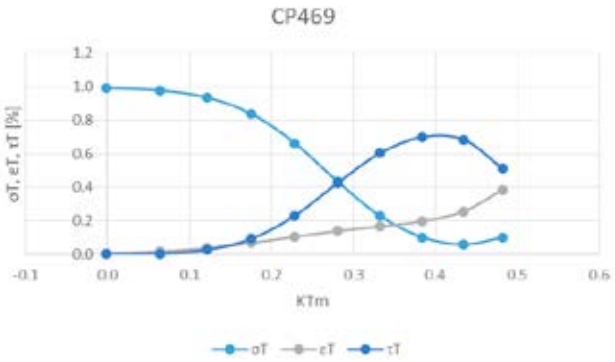

Fig. 7. Uncertainty contributions for propeller CP469

CONCLUSIONS

The following conclusions can be drawn from the results presented in this paper:

- For most of the loading values, the overall uncertainty of $K_{T/Q}$ was below 2% for both propellers.
- For the fixed pitch propeller:
  - The test repeatability plays a dominant role for lower loadings.
  - The bias starts to become important at moderate and higher loadings, but there is no clear trend that can be used to evaluate repeatability/bias domination.
  - The geometry tolerance impact seems to be irrelevant in this case.
- For the controllable pitch propeller:
  - The test repeatability plays a dominant role for lower loadings.
  - The bias has a generally low uncertainty contribution; it is notable at high loadings only.
  - The geometry tolerance impact seems to be irrelevant at lower loadings; however, it becomes dominant at high loadings.
- The fluctuating character of uncertainty contributions in the case of Fixed Pitch Propeller (FPP) may result from the notably lower uncertainty level and the resulting higher sensitivity of the analysed values to small deviations.
- The much higher geometry impact in the case of Controllable Pitch Propeller (CPP) seems to result from the double uncertainty of the propeller pitch: first, at the level of geometry definition, and second, in setting the target pitch.
- The obtained results provide a rational limit for tying the results of numerical calculations to the experimental results.
- Future analyses that incorporate the uncertainties of hull resistance and self-propulsion tests may make it possible to determine the quality of commercially offered powering predictions.

REFERENCES

1. B. Volker, Prac[tical ship hydrodynamics, Butterworth Heinemann, 2000, doi: 10.1016/B978-0-08-097150-6.10007-7.

2. M. Schmiechen, '50 years rational theory of propulsion', *First International Symposium on Marine Propulsors*, Trondheim, 2009.

3. C. Dymarski, 'A concept design of diesel-hydraulic propulsion system for passenger ship intended for inland shallow water navigation', *Polish Maritime Research,* vol. 26, no. 3, pp. 30-38, 2019, doi: 10.2478/pomr-2019-0043.

4. L. Greitsch, M. Druckenbrod, S. Bednarek and H.-J. Heinka, 'A holistic design approach for propulsion packages', *Third International Symposium on Marine Propulsors*, Launceston, 2013.

5. I. Kamal, J. Binns, N. Bose and G. Thomas, 'Reliability assessment of ship powering performance extrapolations using Monte Carlo methods', *Third International Symposium on Marine Propulsors*, Launceston, 2013.

6. N. Bose and M. Susan, 'Reliability and accuracy of ship powering performance extrapolation', *First International Symposium on Marine Propulsors*, Trondheim, 2009.

7. N. Hasuike, M. Okazaki, A. Okazaki and K. Fujiyama, 'Scale effects of marine propellers in POT and self propulsion test conditions', in *Fifth International Symposium on Marine Propulsors*, Espoo, 2017.

8. S.B. Muller, M. Abdel-Maksound and G. Hilbert, 'Scale effects on propellers for large container vessels', *First International Symposium on Marine Propulsors*, Trondheim, 2009.

9. Bugalski T., Streckwall H. and J. Szantyr, 'Critical review of propeller performance scaling methods, based on model experiments and numerical calculations', *Polish Maritime Research*, vol. 20, no. 4, 2013, doi: 10.2478/pomr-2013-0043.

10. S. Helma, S. Heinrich and J. Richter, 'The effect of propeller scaling methodology on the performance prediction', *Fifth International Symposium on Marine Propulsors*, Espoo, 2017.

11. V. Krasilnikov, S. Lucia and S. Kristina, 'Numerical investigation into scale effect on the performance characteristics of twin-screw offshore vessels', *Fifth International Symposium on Marine Propulsors*, Espoo, 2017.

12. N. Bulten and P. Stoltenkamp, 'Full scale CFD; the end of the Froude-Reynolds battle', *Fifth International Symposium on Marine Propulsors*, Espoo, 2017.

13. V. Krasilnikov, 'Self-propulsion RANS computations with a single-screw container ship', *Third International Symposium on Marine Propulsors*, Launceston, 2013.

14. Y. Zhang, X. P. Wu, M. Y. Lai, G. P. Zhou and J. Zhang, 'Feasibility study of RANS in predicting propeller cavitation in behind-hull conditions', *Polish Maritime Research,* vol. 27, no. 4, 2020, doi: 10.2478/pomr-2020-0063.

15. T. Cepowski, 'Regression formulas for the estimation of engine total power for tankers, container ships and bulk carriers on the basis of cargo capacity and design speed', *Polish Maritime Research,* vol. 26, no. 1, 2019, doi: 10.2478/pomr-2019-0010.

16. A. Vrijdag, J. de Jong and H. van Nuland, 'Uncertainty in Bollard pull predictions', *Third International Symposium on Marine Propulsors*, Launceston, 2013.

17. L. Rowiński and M. Kaczmarczyk, 'Evaluation of effectiveness of waterjet propulsor for a small underwater vehicle', *Polish Maritime Research,* vol. 28, no. 4, 2022, doi: 10.2478/pomr-2021-0047.

18. A. Nadery and H. Ghassemi, 'Numerical investigation of the hydrodynamic performance of the propeller behind the ship with and without WED', *Polish Maritime Research,* vol. 27, no. 4, 2020, doi: 10.2478/pomr-2020-0065.

19. M. Burak Samsul, 'Blade cup method for cavitation reduction in marine propellers', *Polish Maritime Research,* vol. 28, no. 2, 2021, doi: 10.2478/pomr-2021-0021.

20. P. Król, 'Blade section profile array lifting surface design method for marine screw propeller blade', *Polish Maritime Research,* vol. 26, no. 4, 2019, doi: 10.2478/pomr-2019-0075.

21. L. Guangnian, Q. Chen and Y. Liu, 'Experimental study on dynamic structure of propeller tip vortex', *Polish Maritime Research,* vol. 27, no. 2, 2020, doi: 10.2478/pom4-2020-022.

22. Propulsion Committee of the 28th ITTC, 'ITTC - Recommended Procedures and Guidelines', ITTC, 2022. [Online]. Available: https://www.ittc.info/media/7977/75-01-02-02.pdf. [Accessed 8 August 2022].

23. Quality Systems Group of the 28th ITTC, 'ITTC - Recommended Procedures and Guidelines', ITTC, 2022. [Online]. Available: https://www.ittc.info/media/8027/75-02-03-022.pdf. [Accessed 8 August 2022].

CONTACT WITH THE AUTHOR

Przemysław Król
e-mail: krolprz30@gmail.com

Maritime Advanced Research Centre
Poland